Sandstone composition of the Upper Jurassic Emuerhe Formation from the Mohe Basin, China

MING MING ZHANG, ZHAO JUN LIU*, SHI FANG & QIU SHI SUN

College of Earth Science, Jilin University, Changchun 130061, China

Abstract – The sandstone composition analysis carried out on the samples from three different sections (western section, middle section and eastern section) of the Upper Jurassic Emuerhe Formation in the Mohe Basin, northeastern China, reveals that the Okhotsk orogenic belt and the Ergun massif basement are the source areas for the Emuerhe Formation. The source area of the western section and the A segment of the middle section is the Okhotsk orogenic belt. The tectonic attributes of the Okhotsk orogenic belt are those of a dissected arc. The transportation distance of clastic rocks from these sections gradually lengthened, and the uplift rate of the Okhotsk orogenic belt gradually increased. The source area of the eastern section and the B segment of the middle section is the Ergun massif basement. Compared with the Okhotsk orogenic belt, the tectonic attributes and uplift rate of the Ergun massif basement are different from the former. The attributes of the Ergun massif basement are those of basement uplift. The transportation distance of clastic rocks from the eastern section and the B segment of the middle section gradually shortened, and the uplift rate of the Ergun massif basement gradually decreased. These conclusions are consistent with the characteristics of a foreland basin. Thus, we can draw the conclusion that the Mohe Basin belongs to the foreland basin.

Keywords: Mohe Basin, Upper Jurassic, Emuerhe Formation, sandstone composition, tectonic implications.

1. Introduction

The Mohe Basin is located in the northeast of China, which has huge hydrocarbon generation potential (Wu, Wang & Yang, 2004). Previous studies showed that the Mohe Basin was formed under the influence of the closure of the ancient Okhotsk Ocean (He *et al*. 2003; Hou *et al*. 2010*a,b*). The formation ages and the basin trends of the Mohe Basin are markedly different from the other basins in the northeast of China. These characteristics indicate that there are different formation mechanisms between the Mohe Basin and the other basins in this area (He *et al*. 2003; Hou *et al*. 2010*a,b*). Therefore, studies on the Mohe Basin can provide the basis for research on the regional tectonic evolution history and basin analysis in this area.

The Emuerhe Formation is the most important sedimentary deposit of the Mohe Basin. The basin's expansion and the sedimentary thickness accumulated during the deposition of the Emuerhe Formation are both the largest (Xin, Wu & Yang 2003). Hence, the Emuerhe Formation can act as an important record for the study of the tectonic attributes of the source areas and the sedimentary evolution history of the Mohe Basin. Previous studies have made some achievements in discerning the sedimentary features and source provenance of the whole of the Upper Jurassic through the use of field outcrops, geochemistry and seismic analyses (Zhang *et al*. 2003; Wu *et al*. 2006; He, Wang &

Hou, 2008; Hou *et al*. 2010*a,b*;). However, they did not clarify the source areas of the Emuerhe Formation. In addition, they did not study the uplift rate and the tectonic attributes of the source areas or the transportation distance of the clastic rocks. Sandstone petrography is of great significance in the study of the formation mechanisms of basins and the tectonic evolution history of the source areas (Morton & Hallsworth, 1994; Gray & Zeitler, 1997; Yan *et al*. 2002; Marenssi, Net & Santillana, 2002). In this work, the tectonic implications (source areas of each section, tectonic attributes and uplift rate of the source areas, transportation distance of clastic sediments, and attributes of the Mohe Basin) of the sandstone composition of the Emuerhe Formation can be analysed through the sandstone petrography of the selected samples. Thus, the geodynamic and palaeogeographic significance of this region can be interpreted.

2. Geological setting

The Mohe Basin is located to the north of the Ergun massif and to the south of the Okhotsk orogenic belt. Many E–W-trending faults were developed in the Mohe Basin. However, S–N-trending faults were rarely developed in it. This phenomenon may be caused by the collision of the Ergun massif and the Okhotsk orogenic belt. The entire succession of the Mohe Basin is constituted by a sedimentary cover overlying the basement rocks. The basement rocks are mainly composed of the
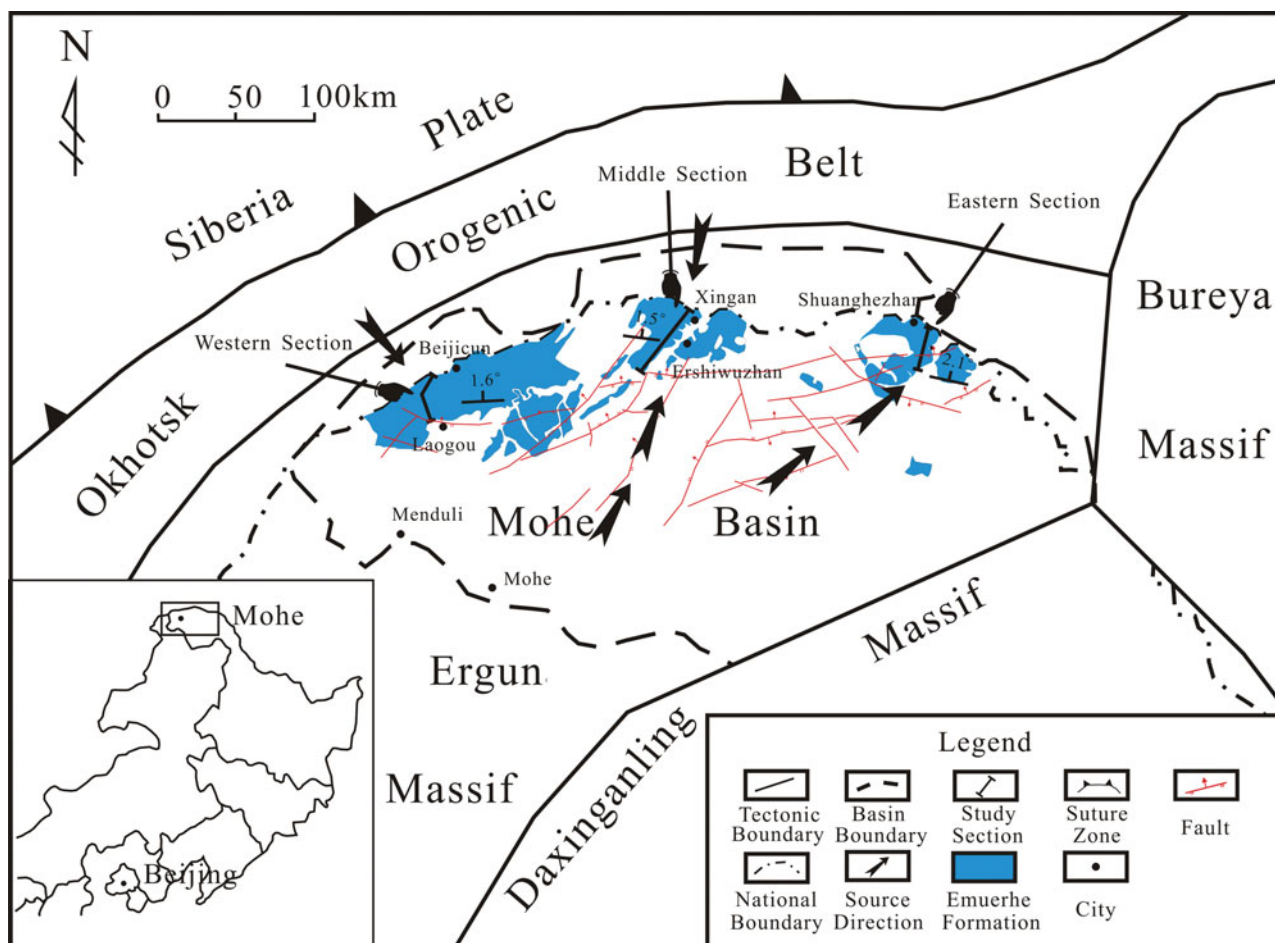
*Author for correspondence: 915824051@qq.com

Figure 1. (Colour online) Geological sketch maps of the studied area with location of the studied sections (modified from Xie, 2000; Hou *et al*. 2010*a*).

metamorphic rocks of the Proterozoic Xinghuadukou Group, the sedimentary rocks of the Devonian Niqiuhe Formation and Palaeozoic granite. The sedimentary cover is mainly composed of Upper Jurassic terrigenous clastic rocks (the Xiufeng Formation, the Ershierzhan Formation, the Emuerhe Formation and the Kaikukang Formation) and Cretaceous volcanic rocks (Wu *et al*. 2003; Xin, Wu & Yang, 2003). The Upper Jurassic Emuerhe Formation is mainly composed of terrigenous clastic rocks. Its lower part is mainly composed of fine sandstone, medium-grained sandstone and coarse sandstone sometimes interbedded with conglomerate and siltstone, and the upper part is mainly composed of fine sandstone, medium-grained sandstone and mudstone. Some coarse sandstone interlayers occasionally occur. Some gastropods, ostracods, plants and sporopollen fossils can be found in this formation. In addition, the Emuerhe Formation is mainly distributed in the Laogou, Beijicun, Xingan, Ershiwuzhan and Shuanghezhan areas (Fig. 1).

3. Methodology

According to the characteristics of the Emuerhe Formation in the Mohe Basin, three stratigraphic sections were selected as the study areas, respectively named the western section, the middle section and the eastern section. The main sedimentary facies of these sections are lake facies and fan delta facies. The western section is 872 m thick. Its lower part is mainly constituted by medium–coarse-grained sandstone sometimes interbedded with fine sandstone. The upper part is mainly constituted by fine sandstone and mudstone. The middle section is 1186 m thick. Its lower part is mainly constituted by fine sandstone, medium-grained sandstone and coarse sandstone. The upper part is mainly constituted by fine sandstone and mudstone. The eastern section is 947 m thick. Its lower part and upper part are all mainly constituted by fine sandstone and medium-grained sandstone sometimes interbedded with mudstone. The sampling locations are shown in Figure 2.

Twelve, sixteen and nine sandstone samples were collected from the western section, the middle section and the eastern section, respectively. The rock types of the samples collected from the Emuerhe Formation sections are mainly fine sandstones, medium-grained sandstones and coarse sandstones. On average, over 350 points were counted in each thin-section. The modal composition data obtained from the Emuerhe Formation samples are given in Table 1. All the samples are classified after Folk (1974).
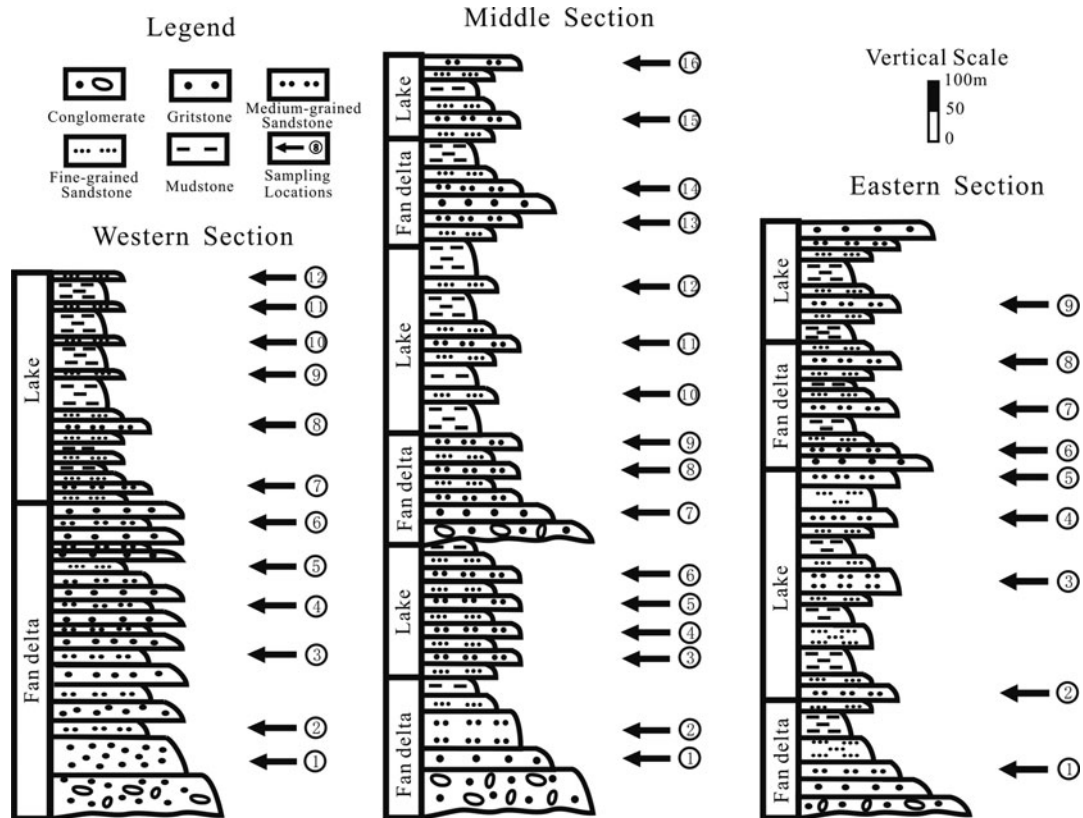
Figure 2. Stratigraphic sections of the Emuerhe Formation with location of the studied samples.

4. Sandstone petrology and detrital modes

The sandstone grains of the western section samples are angular and sub-angular, and are moderately sorted. The grain size is 0.5–1.2 mm. Matrix content is 3–6 %. The sandstones are grain-supported, ranging from arkose to lithic arkose (Figs 3a, b, 4a). The quartz content ranges from 27.6 % to 47.8 % (average = 36.5 %). Monocrystalline quartz is present in a higher percentage than polycrystalline quartz. The feldspar content ranges from 38.8 % to 48.6 % (average = 44.3 %), and is composed of K-feldspar and plagioclases. Plagioclases and K-feldspar are present in equal amounts. Some detrital feldspar was partially dissolved and/or replaced by kaolinite or sericite. The rock fragment content ($Lv + Ls + Lm$) ranges from 13.4 % to 24 % (average = 19.23 %), and is mainly sandstone debris, carbonate debris, andesite debris and mylonite debris. Among these three types of rock fragments, the percentage of igneous rock fragments is the highest. The percentage of sedimentary rock fragments is smaller than the former. The percentage of metamorphic rock fragments is the lowest.

The sandstone grains of the middle section samples are angular and are moderately sorted. The grain size is 0.3–1.0 mm. The matrix content is 4–6 %. The sandstones are grain-supported, ranging from arkose to lithic arkose (Figs 3c, d, 4b). Quartz content ranges from 28.9 % to 51.4 % (average = 37.86 %). Monocrystalline quartz is present in a higher percentage

than polycrystalline quartz. The feldspar content ranges from 41.1 % to 60.5 % (average = 50.24 %), and is composed of K-feldspar and plagioclases. Plagioclases are present in a higher percentage than K-feldspar. Some detrital feldspar was partially dissolved and/or replaced by kaolinite or sericite. The rock fragment content ranges from 5.7 % to 23.9 % (average = 11.96 %), and is mainly sandstone debris, carbonate debris, granite debris, andesite debris, quartz schist debris, phyllite debris and mylonite debris. Among these three types of rock fragments, the percentage of igneous rock fragments is the highest. The percentage of sedimentary rock fragments is smaller than the former. The percentage of metamorphic rock fragments is the lowest. In addition, the extrusive rock fragments (andesite debris) can only be found in the A segment of the middle section (samples 1–6), and are not found in the B segment (samples 7–16).

The sandstone grains of the eastern section samples are angular and sub-angular, and are moderately sorted. The grain size is 0.3–0.8 mm. The matrix content is 5–8 %. The sandstones are grain-supported arkose (Figs 3e, f, 4c). The quartz content ranges from 32.3 % to 50.1 % (average = 41.74 %). Monocrystalline quartz is present in a higher percentage than polycrystalline quartz. The feldspar content ranges from 43.8 % to 57.1 % (average = 49.98 %), and is composed of K-feldspar and plagioclases. K-feldspar is present in a higher percentage than plagioclases. Some detrital feldspar was also partially dissolved and/or replaced by

Table 1. Sandstone composition of the Emuerhe Formation in the Mohe Basin

Section	Sample number	Qm	Qp	Qt	P	K	F	Lt	L	Lv intrusive	Lv extrusive	Lv	Ls	Lm
Western section	1	25.7	3.8	29.5	24.7	21.8	46.5	27.8	24.0	6.1	8.1	14.2	6.3	3.5
	2	26.2	1.4	27.6	26.3	22.3	48.6	25.2	23.8	6.3	7.8	14.1	5.8	3.9
	3	28.6	3.7	32.3	23.7	21.5	45.2	26.2	22.5	5.9	7.7	13.6	5.7	3.2
	4	31.5	5.8	37.3	23.3	21.6	44.9	23.6	17.8	3.9	6.6	10.5	4.6	2.7
	5	29.4	2.7	32.1	24.5	22.2	46.7	23.9	21.2	5.6	7.2	12.8	5.4	3.0
	6	32.1	5.4	37.5	23.6	22.0	45.6	22.3	16.9	4.0	6.3	10.3	4.2	2.4
	7	29.6	4.8	34.4	23.0	21.8	44.8	25.6	20.8	5.5	7.2	12.7	5.3	2.8
	8	31.9	5.9	37.8	22.2	21.3	43.5	24.6	18.7	5.1	7.1	12.2	4.4	2.1
	9	33.4	6.7	40.1	21.5	20.7	42.2	24.4	17.7	5.2	6.4	11.6	3.9	2.2
	10	34.9	5.1	40.0	21.1	20.5	41.6	23.5	18.4	5.4	7.0	12.4	3.6	2.4
	11	34.6	7.2	41.8	21.8	20.8	42.6	22.8	15.6	4.2	6.7	11.9	2.5	1.2
	12	38.9	8.9	47.8	20.8	18.0	38.8	22.3	13.4	4.1	6.1	10.2	2.5	0.7
Middle section	1	27.6	2.3	29.9	24.6	21.6	46.2	26.2	23.9	6.2	7.4	13.6	6.2	4.1
	2	29.7	2.7	32.4	23.5	22.5	46.0	24.3	21.6	5.6	6.8	12.4	5.6	3.6
	3	33.5	3.8	37.3	25.0	22.1	47.1	19.4	15.6	4.3	4.2	8.5	4.7	2.4
	4	33.6	3.0	36.6	22.6	21.2	43.8	22.6	19.6	5.3	6.3	11.6	4.9	3.1
	5	37.2	4.1	41.3	21.7	19.4	41.1	21.7	17.6	4.8	5.7	10.5	4.2	2.9
	6	38.6	4.8	43.4	22.3	21.9	44.2	17.2	12.4	3.7	4.2	7.9	3.4	1.1
	7	46.9	4.5	51.4	34.6	9.3	43.9	10.2	5.7	4.3	0.0	4.3	1.0	0.4
	8	45.2	4.0	49.2	34.8	10.1	44.9	9.9	5.9	4.5	0.0	4.5	1.4	0.0
	9	42.7	3.4	46.1	36.5	11.1	47.6	9.7	6.3	5.1	0.0	5.1	0.8	0.4
	10	36.3	2.9	39.2	39.6	14.1	53.7	10.0	7.1	5.4	0.0	5.4	1.2	0.5
	11	34.7	3.1	37.8	38.7	15.3	54.0	11.3	8.2	5.2	0.0	5.2	1.4	1.6
	12	33.3	2.5	35.8	39.9	16.4	56.3	10.4	7.9	4.6	0.0	4.6	1.8	1.5
	13	30.5	2.1	32.6	40.5	17.6	58.1	11.4	9.3	5.1	0.0	5.1	2.3	1.9
	14	32.4	2.3	34.7	40.8	15.9	56.7	10.9	8.6	6.0	0.0	6.0	1.4	1.2
	15	27.3	1.8	29.1	42.3	18.2	60.5	12.2	10.4	6.5	0.0	6.5	2.2	1.7
	16	27.7	1.2	28.9	41.2	18.6	59.8	12.5	11.3	6.1	0.0	6.1	3.1	2.1
Eastern section	1	43.5	6.6	50.1	35.7	8.1	43.8	12.7	6.1	4.2	0.0	4.2	0.0	1.9
	2	43.1	6.7	49.8	35.9	8.9	44.8	12.1	5.4	3.6	0.0	3.6	0.4	1.4
	3	38.5	4.8	43.3	39.5	9.4	48.9	12.6	7.8	5.1	0.0	5.1	0.3	2.4
	4	39.4	4.4	43.8	38.6	9.3	47.9	12.7	8.3	5.3	0.0	5.3	0.7	2.3
	5	37.7	3.9	41.6	40.1	9.7	49.8	12.5	8.6	5.2	0.0	5.2	0.7	2.7
	6	34.7	4.1	38.8	41.8	10.3	52.1	13.2	9.1	5.2	0.0	5.2	0.8	3.1
	7	36.6	3.7	40.3	41.0	9.9	50.9	12.5	8.8	5.1	0.0	5.1	0.8	2.9
	8	33.3	2.4	35.7	42.8	11.8	54.6	12.1	9.7	5.5	0.0	5.5	1.0	3.2
	9	31.1	1.2	32.3	43.9	13.2	57.1	11.8	10.6	5.8	0.0	5.8	1.3	3.5

Symbols: Qm – monocrystalline quartz; Qp – polycrystalline quartz; Qt – total quartzose grains (Qm + Qp); P – plagioclases; K – K-feldspar; F – total feldspar grains (P + K); Lv – volcanic–metavolcanic rock fragments ($Lv_{extrusive} + Lv_{intrusive}$); $Lv_{extrusive}$ – extrusive rock fragments; $Lv_{intrusive}$ – intrusive rock fragments; Ls – sedimentary rock fragments; Lm – metasedimentary rock fragments; L – lithic fragments (Lv + Ls + Lm). Lt – (Lv + Ls + Lm + Qp).

kaolinite or sericite. The rock fragment content ranges from 5.4 % to 10.6 % (average = 11.96 %), and is mainly sandstone debris, granite debris, quartz schist debris and phyllite debris. Among these three types of rock fragments, the percentage of igneous rock fragments is the highest. The percentage of metamorphic rock fragments is smaller than the former. The percentage of sedimentary rock fragments is the lowest. In addition, the extrusive rock fragments (andesite debris) were not found in this section either.

5. Tectonic implications

Tectonic activity frequently took place in the Mohe Basin and in the surrounding areas during the Late Jurassic (Zhang *et al*. 2003; Wu *et al*. 2006; Chang *et al*. 2007; Li, 2007). In such an environment, the accumulation rate of the sediment is fast, so the sandstone composition is determined by the lithology of the source areas and the transportation distance of the clastic rocks. Previous studies showed that sandstone composition has been successfully applied to the ana-

lysis of geological features, such as the source direction, provenance tectonic setting and uplift rate (Ingersoll & Suczek, 1979; Ingersoll *et al*. 1984; Ingersoll, 1988; Graham *et al*. 1993; Hendrix, 2000; Li *et al*. 2004*a,b*; Rieser *et al*. 2005; Fang *et al*. 2006, 2007*a,b*; Critelli *et al*. 2008, 2013; Perri *et al*. 2008, 2011, 2012, 2013; Zaghloul *et al*. 2010; Ghazi & Mountney, 2011; Caracciolo *et al*. 2011). In this work, the features of the source areas and the tectonic uplift processes that occurred during the Late Jurassic have been studied via the sandstone composition analysis of the Emuerhe Formation from the Mohe Basin.

5.a. Inverse sequence section analysis

An inverse sequence section refers to the phenomenon in which the stratigraphic sequence in the basin is the opposite to the stratigraphic sequence in the orogenic belt, which means that the older strata in the orogenic belt correspond to the younger strata in the basin, and the younger strata in the orogenic belt correspond to the older strata in the basin. Previous studies have shown
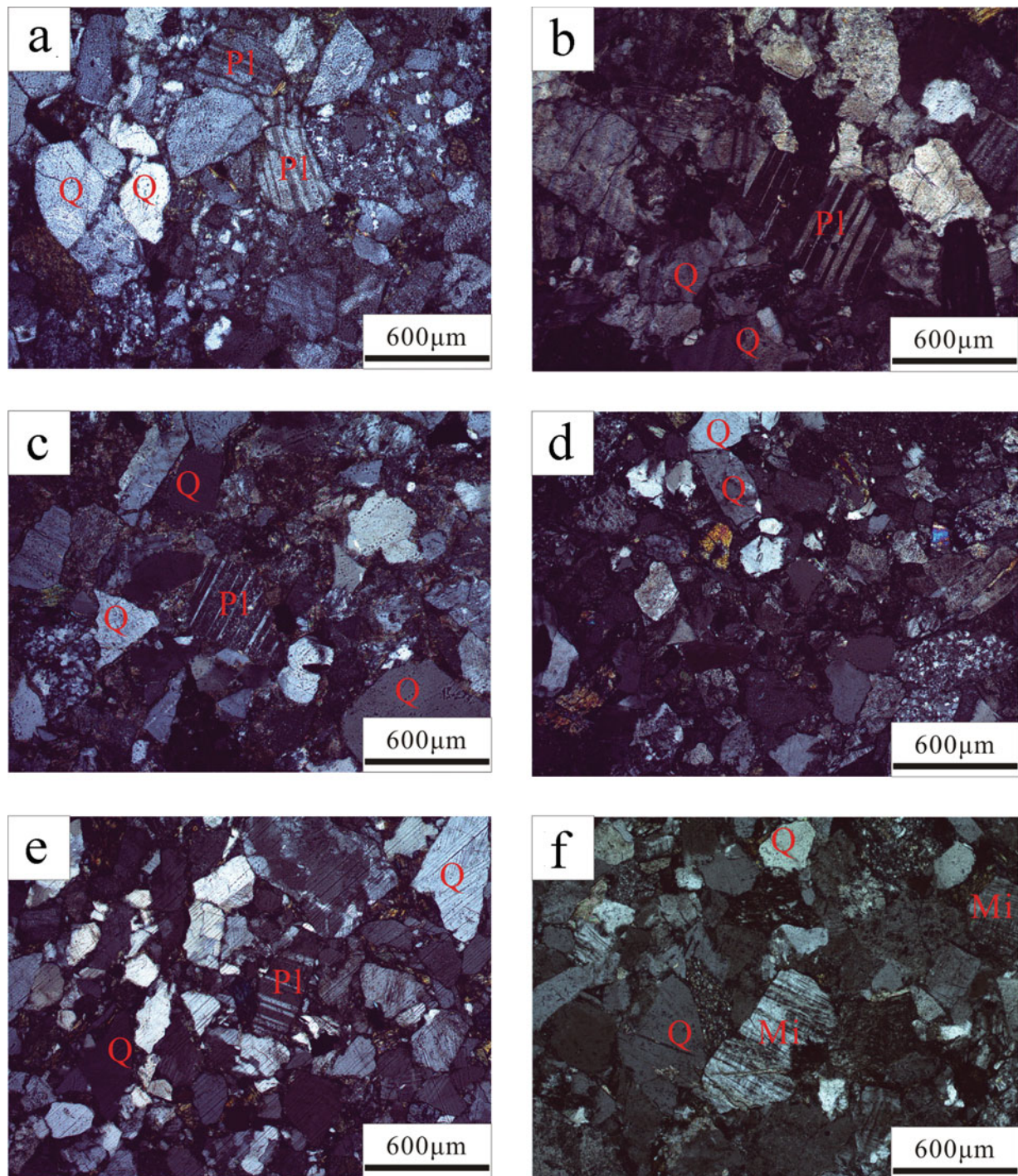
Figure 3. (Colour online) Photomicrographs of sand grains of the Emuerhe Formation: (a) lithic arkose sandstones from the western section; (b) arkosic sandstones from the western section; (c) arkosic sandstones from the middle section; (d) lithic arkose sandstones from the middle section; (e) arkosic sandstones from the eastern section; (f) arkosic sandstones from the eastern section. (Q – quartz; Pl – plagioclase; Mi – microcline.)

that the possible source areas for the whole Upper Jurassic strata in the Mohe Basin consist of a northern source area and a southern source area (He, Wang & Hou, 2008; Hou *et al*. 2010*a*,*b*). The northern source area is the Okhotsk orogenic belt on the southern margin of the Siberian plate. The stratigraphic sequence of the Okhotsk orogenic belt is made up of Precambrian metamorphic crystalline basement (such as mylonite and phylonite), Cambrian volcano-siliceous rocks, Silurian

extrusive rocks and granite, marine carbonate deposits (Devonian, Carboniferous and Permian in age), and continental sandstone and conglomerate (Early Jurassic) (Xu & Yan, 1996; Mo, Han & Li, 2005; Wang *et al*. 2009; Shao *et al*. 2011). The southern source area is the Ergun massif basement. The stratigraphic sequence of the Ergun massif basement is made up of Precambrian Xinghuadukou Group metamorphic rocks (such as quartz schist and phyllite), Cambrian granite,
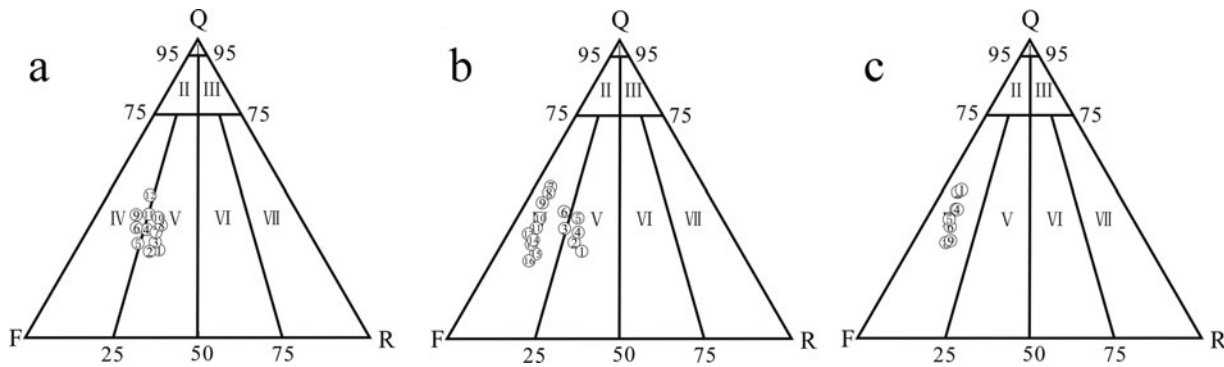
Figure 4. Mineralogical classification of the Emuerhe Formation sandstones based on the Folk diagram (1974): Q – total quartz; F – feldspar; R – rock fragments. I – quartz sandstone; II – feldspathic quartz sandstone; III – lithic quartz sandstone; IV – arkosic sandstone; V – lithic arkose sandstone; VI – feldspar lithic sandstone; VII – lithic sandstone. The rock classification names are modified from Zeng & Xia (1998) and Lu & Sang (2002). Figure A: Sandstone components classification for the sandstones from the western section; Figure B: Sandstone components classification for the sandstones from the middle section; Figure C: Sandstone components classification for the sandstones from the eastern section.

terrigenous sedimentary socks (Silurian and Triassic in age), and continental sandstone and conglomerate (Early Jurassic) (Sun, Li & Zhang, 2002; Wu *et al.* 2005; Hou *et al.* 2010*a,b*).

The sandstone debris (Fig. 5–1), carbonate debris (Fig. 5–2), andesite debris (Fig. 5–3) and mylonite debris (Fig. 5–4) occurred in that order in the western section from the bottom to the top. The sequence of the rock fragments in the A segment of the middle section is same as that in the western section. The sandstone debris (Fig. 5–5), carbonate debris (Fig. 5–6), andesite debris (Fig. 5–7) and mylonite debris (Fig. 5–8) occurred in that order in the A segment of the middle section from the bottom to the top. However, the sequence of the rock fragments in the B segment of the middle section is different from the A segment. The sandstone debris (Fig. 5–9), granite debris (Fig. 5–10) and quartz schist debris (Fig. 5–12) occurred in that order in the B segment from the bottom to the top. In addition, quartz with wavy extinction only occurred in the upper part of the B segment (Fig. 5–11), which means that this kind of quartz mainly comes from the metamorphic rocks. The sandstone debris (Fig. 5–13), granite debris (Fig. 5–14), quartz schist debris (Fig. 5–15) and phyllite debris (Fig. 5–16) occurred in that order in the eastern section from the bottom to the top.

The debris characteristics of the western section are similar to the A segment of the middle section. Sedimentary rock debris (carbonate debris) constitutes the base of the section, whereas the mylonite fragments are mainly distributed at the top. The Okhotsk orogenic belt basement is composed of metamorphic rocks (mylonite and phylonite), whereas the upper part is mainly composed of marine carbonate, which means that the stratigraphic sequence of the western section and the A segment of the middle section is opposite to the stratigraphic sequence of the Okhotsk orogenic belt. The sequence of the rock fragments in the B segment of the middle section is the same as that in the eastern

section. Sedimentary rock debris constituted the base of the section; quartz schist debris and phyllite debris are mainly distributed at the top. The lower part of the Ergun massif basement is composed of metamorphic rocks (quartz schist and phyllite), and the upper part is mainly composed of sedimentary rocks, which means that the stratigraphic sequence of the eastern section and the B segment of middle section is the opposite to the stratigraphic sequence of the Ergun massif basement. In addition, previous studies have indicated that the extrusive rocks (andesite) did not occur in the southern areas of the Mohe Basin before the Late Jurassic (Hou *et al.* 2010*a,b*). Thus, the extrusive rock debris (andesite debris) is also an important stratigraphic marker between the northern source areas and the southern source areas. The above statistical analysis shows that the extrusive rock debris (andesite debris) only occurred in the western section and the A segment of the middle section, and cannot be found in the B segment of the middle section and the eastern section. Therefore, it is speculated that the Okhotsk orogenic belt is the source area of the western section and the A segment of the middle section, and the Ergun massif basement may be the source area of the eastern section and the B segment of the middle section.

Furthermore, Hou *et al.* (2010*a,b*) used geochemistry, sedimentary facies and seismic methods to analyse the source direction of the whole Upper Jurassic stratum. In these ways he proved that the source direction of the western areas is mainly from the northwest, and the middle areas have two source directions, respectively, to the north and to the south. The source direction of the eastern area is from the southwest (Fig. 1). These results are consistent with the conclusions of this paper.

5.b. Provenance tectonic setting

Sandstone composition analysis is a valuable method to distinguish the provenance tectonic attributes. Thus, the
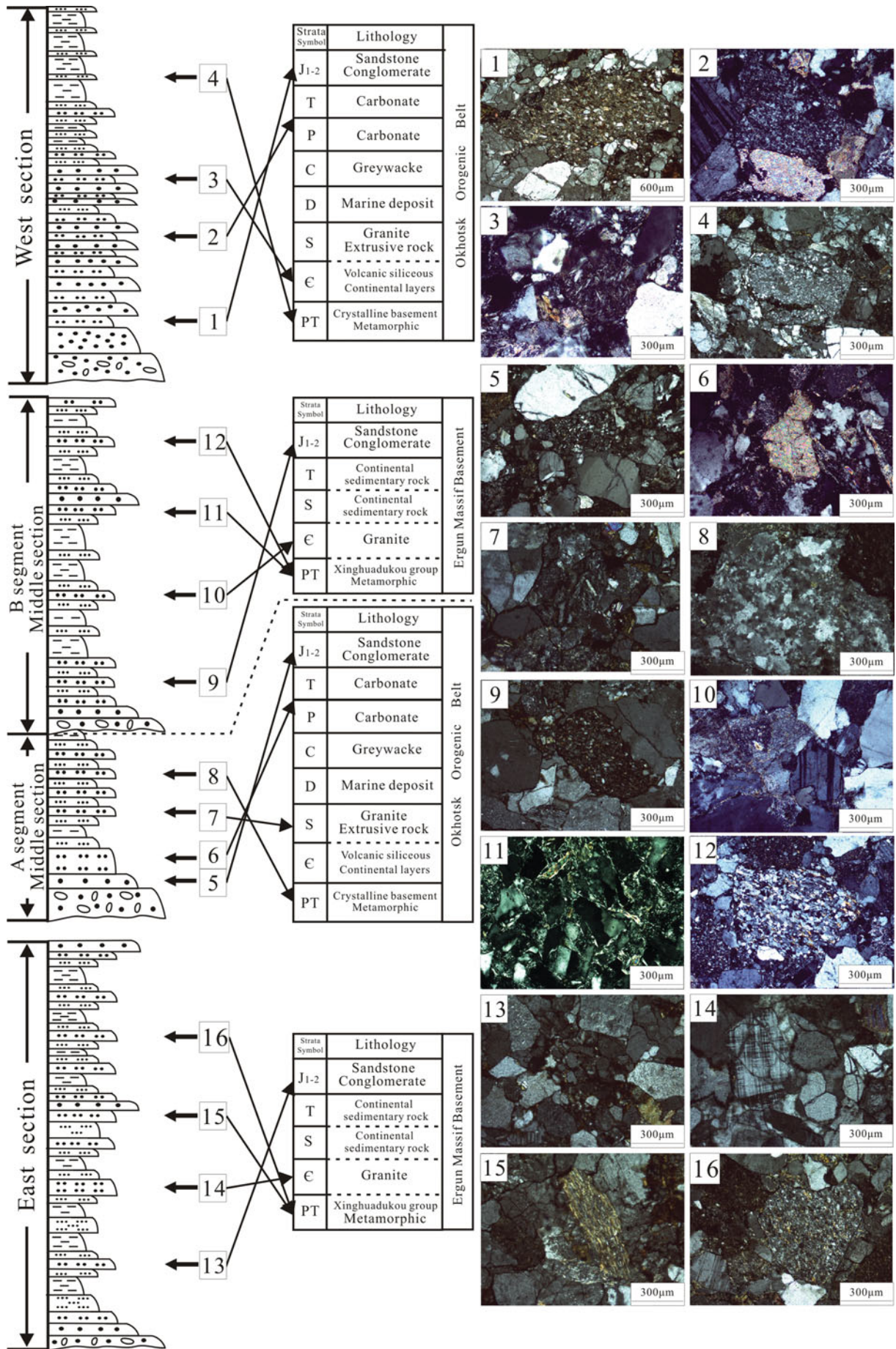
Figure 5. (Colour online) The inverse sequence section relationship between the Emuerhe Formation stratigraphic sections and the source areas.
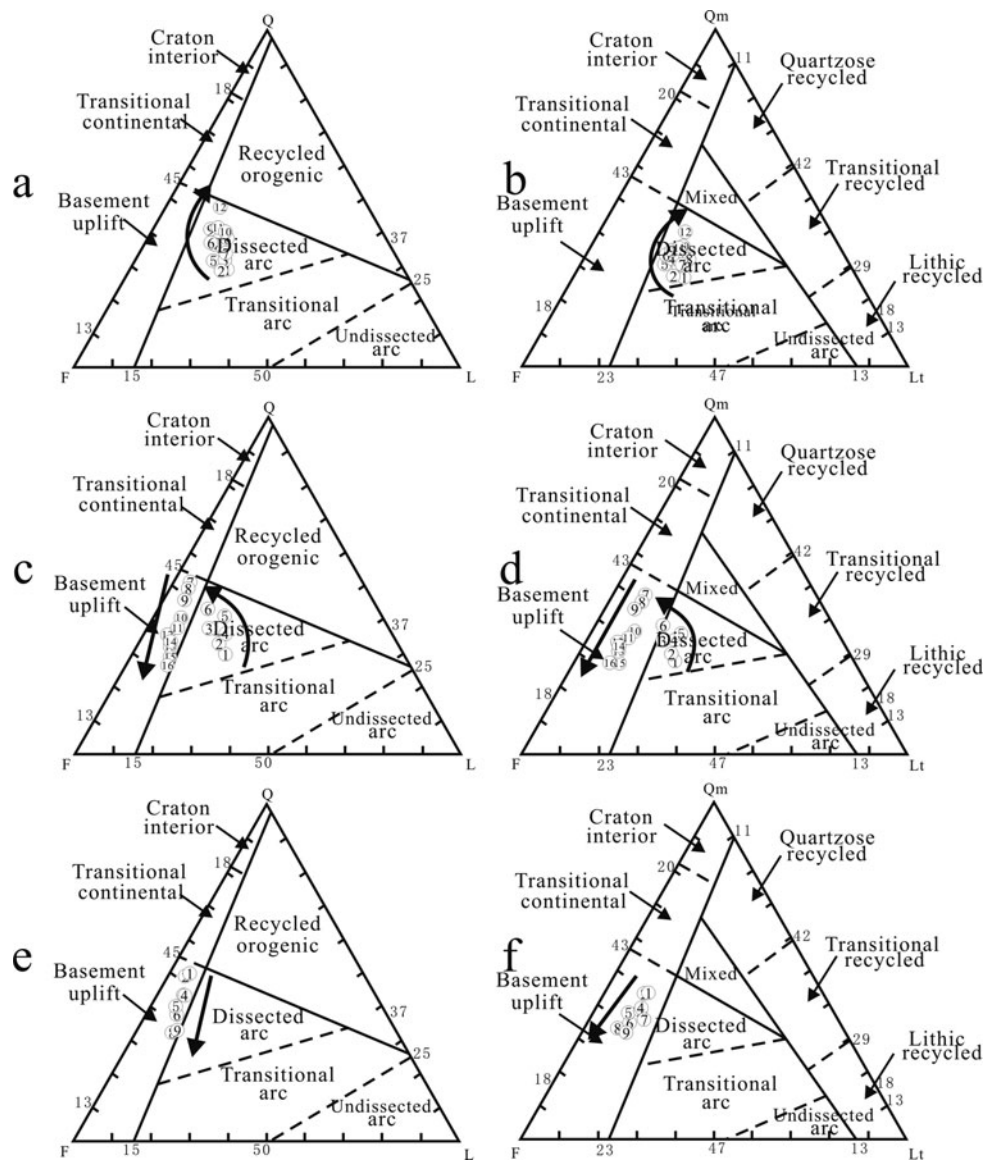
Figure 6. Triangular diagrams of the sandstones from the Emuerhe Formation in Mohe Basin. (a, c, e) Framework-grain assemblage Q–F–L. (b, d, f) Framework-grain assemblage Qm–F–Lt. Tectonic setting fields are from Dickinson (1988). (a, b) Samples form the western section. (c, d) Samples form the middle section. (e, f) Samples form the middle section.

Q–F–L and Qm–F–Lt diagrams (Dickinson & Suczek, 1979; Dickinson *et al.* 1983; Dickinson., 1985, 1988; Critelli & Ingersoll, 1994, 1995) are used to analyse and discuss the provenance tectonic attributes of the Emuerhe Formation.

Samples from the western section fall in the dissected arc field of the Q–F–L diagram (Fig. 6a, b). The Qm–F–Lt plots of the sandstones from the western section show the same results as the Q–F–L diagram. The sandstones (samples 1–6) from the A segment of the middle section fall in the dissected arc field of the Q–F–L and Qm–F–Lt diagrams. However, the sandstones (samples 7–16) from the B segment of the middle section fall in the basement uplift field of the Q–F–L and Qm–F–Lt diagrams (Fig. 6c, d). The sandstones from the eastern section are similar to the samples from the B segment of the middle section, falling in the base-

ment uplift field of the Q–F–L and Qm–F–Lt diagrams (Fig. 6e, f).

Thus, the tectonic attributes of the Okhotsk orogenic belt are those of a dissected arc, whereas the Ergun massif basement has those of basement uplift. These conclusions are in accordance with previous studies based on the geochemistry, zircon U–Pb age and other methods (Crosdale *et al.* 2002; Sun, Li & Zhang, 2002; Ge *et al.* 2005, 2007; Wu *et al.* 2005; Biao, Zheng & Zhou, 2012).

5.c. Vertical variation of sandstone composition

The sandstone clastic components are the result of the uplift and weathering processes of the source areas, which can be used to distinguish the uplift rate of the source areas and the transportation distance of
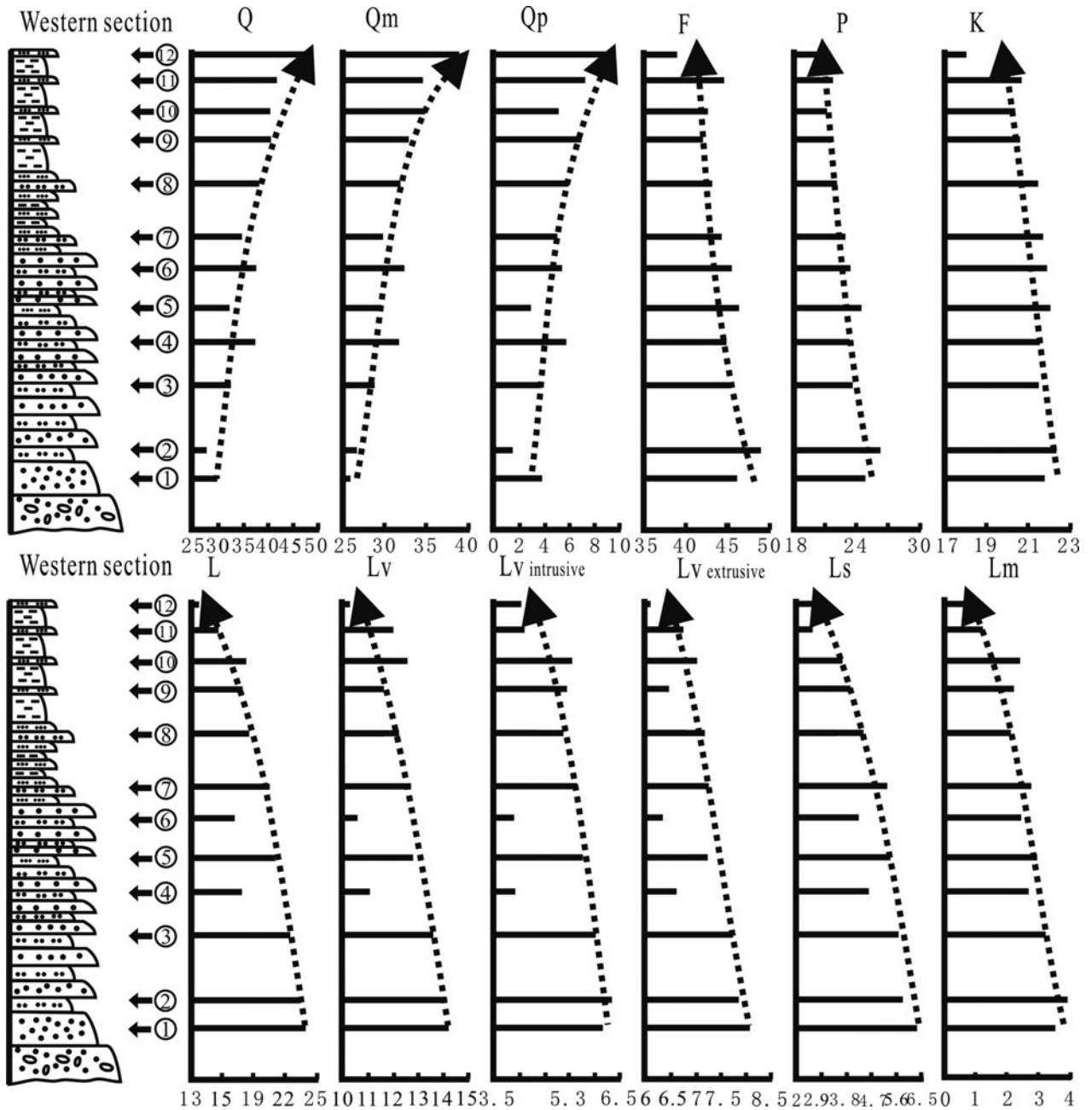
Figure 7. Vertical variation of sandstone components from the Emuerhe Formation in the western section.

the clastic rocks (Critelli *et al.* 2008, 2013; Zaghloul *et al.* 2010; Caracciolo *et al.* 2011; Perri *et al.* 2012, 2013). Generally, the sandstones containing a lot of unstable components (debris and feldspar) and a minor amount of stable components (quartz) are the result of the clastic rocks undergoing a short transportation distance, implying that the uplift rate of the source area is slow. Conversely, the sandstones containing a lot of stable components (quartz) and a minor amount of unstable components (debris and feldspar) are the result of the clastic rocks undergoing long-distance transportation, which means that uplift rate of the source area is fast (Hendrix *et al.* 1992, 2000; Graham *et al.* 1993; Lee & Sheen, 1998; Liu *et al.* 2004; Lin *et al.* 2012).

The content of Qm and Qp increases in the western section and in the A segment of the middle section from the bottom to top. Nevertheless, the content of F, P, K, L, Lv, Lv$_{extrusive}$, Lv$_{intrusive}$, Ls and Lm decreases from bottom to top (Figs 7, 8). Thus, it is speculated that the uplift rate of the Okhotsk orogenic belt gradually increased, and the transportation distance of the clastic rocks gradually lengthened during the deposition period of the Emuerhe Formation. Compared with the western section and the A segment of the middle section, the sandstone composition of the eastern section and the B segment of the middle section shows an opposite trend. The content of Qm and Qp decreases from bottom to top, whereas the content of F, P, K, L,
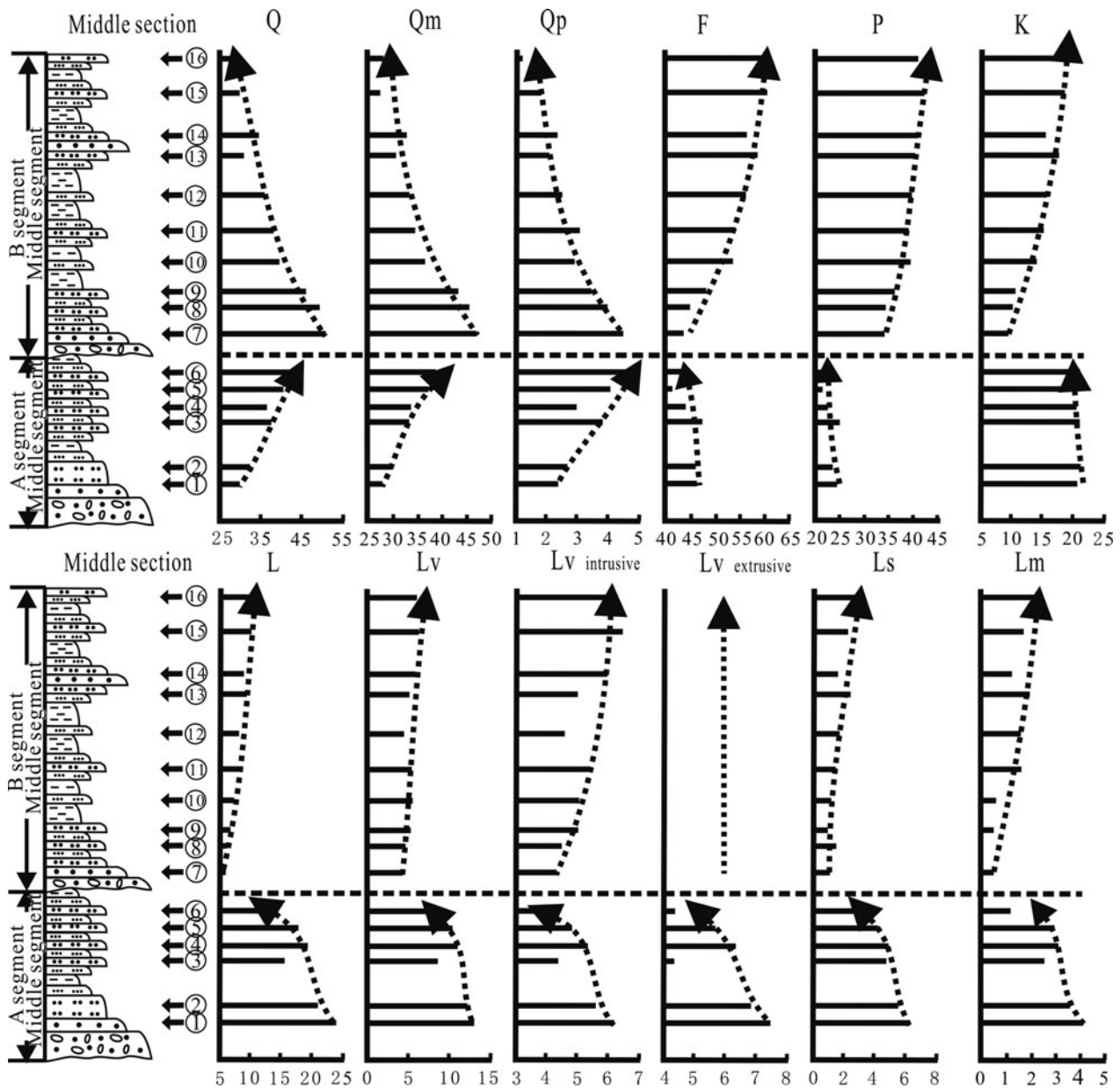
Figure 8. Vertical variation of sandstone components from the Emuerhe Formation in the middle section.

Lv, Lv$_{extrusive}$, Lv$_{intrusive}$, Ls and Lm increases from the bottom to top (Figs 8, 9). Thus, it is speculated that the uplift rate of the Ergun massif basement gradually decreased, and the transportation distance of the clastic rocks gradually shortened during the deposition period of the Emuerhe Formation.

6. Discussion

The source area of the western section is the Okhotsk orogenic belt (Fig. 10a). The transportation distance of the clastic rocks from this section gradually lengthened, and the uplift rate of the Okhotsk orogenic belt gradually increased. The source area of the A segment of the middle section is the Okhotsk orogenic belt as well. The transportation distance of the clastic rocks from this section gradually lengthened, and the uplift rate of the

Okhotsk orogenic belt gradually increased (Fig. 10b). Nevertheless, the source area of the B segment of the middle section is different from the A segment. Its source area is the Ergun massif basement. The transportation distance of the clastic rocks from this segment gradually shortened, and the uplift rate of the Ergun massif basement gradually decreased (Fig. 10b). The source area of the eastern section is the Ergun massif basement as well. The transportation distance of clastic rocks from this section gradually shortened, and the uplift rate of the Ergun massif basement gradually decreased (Fig. 10c).

Generally, the foreland basin on both sides is, respectively, orogenic zone and forebulge area. Moreover, the uplift rate of the orogenic zone increases, whereas the uplift rate of the forebulge area decreases. The phenomenon that the uplift rate of the Okhotsk orogenic
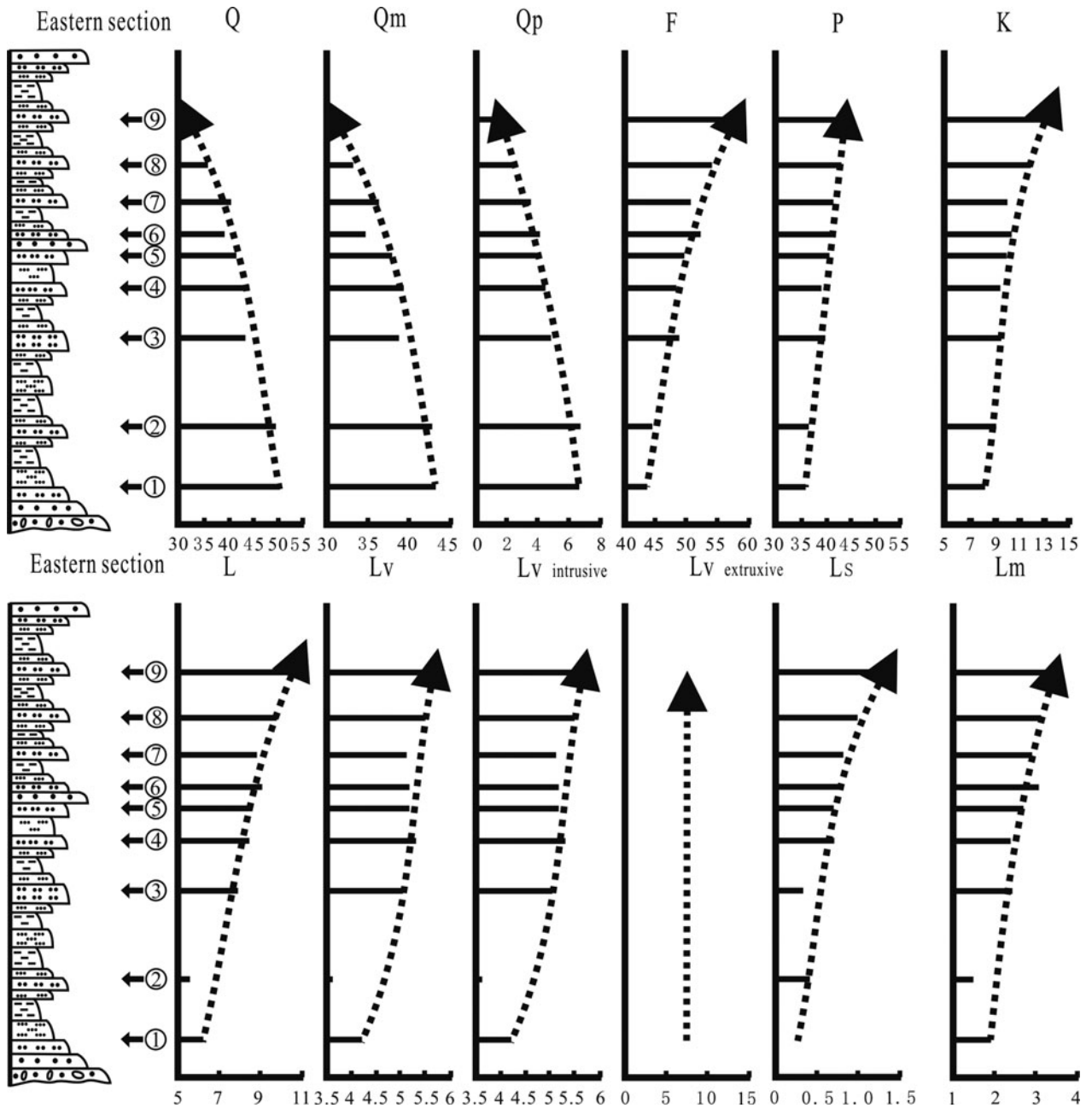
Figure 9. Vertical variation of sandstone components from the Emuerhe Formation in the eastern section.

belt gradually increased and the uplift rate of the Ergun massif basement gradually decreased is consistent with the characteristics mentioned above. Thus, we can draw the conclusion that Mohe Basin should belong to the foreland basin.

7. Conclusions

(1) The source area of each section in the Mohe Basin during the deposition of the Emuerhe Formation is further proved by the inverse sequence section analysis. The source area of the western section and the A segment of the middle section is the Okhotsk orogenic belt, whereas the source area of the eastern section and the B segment of the middle section is the Ergun massif basement.

(2) The tectonic attributes of the Okhotsk orogenic belt are those of a dissected arc. In contrast, the tectonic attributes of the Ergun massif basement are those of basement uplift.

(3) The transportation distance of clastic rocks from the western section and the A segment of the middle section gradually lengthened and the uplift rate of the Okhotsk orogenic belt gradually increased. However, the transportation distance of the clastic rocks from the eastern section and the B segment of the middle section gradually shortened and the uplift rate of the Ergun massif basement gradually decreased.
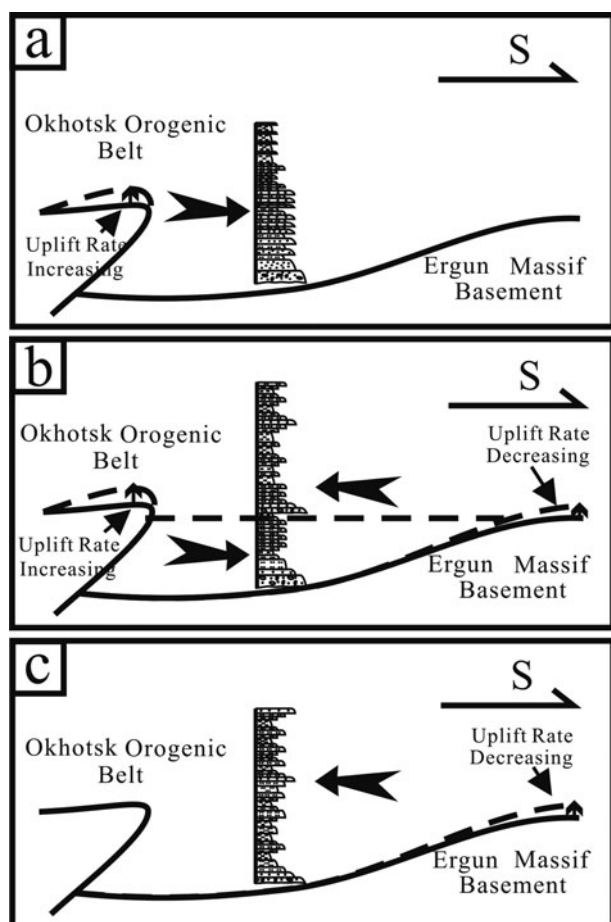
Figure 10. Schematic sketch of provenance analysis of the sandstones from the Emuerhe Formation in the Mohe Basin.

References

BIAO, S. H., ZHENG, W. Z. & ZHOU, X. F. 2012. Zircon U-Pb age of the North Da Hinggan Mts., NE China and its constraint to attribute of the Erguna Block. *Acta Geologica Sinica* **86**, 1262–71 (in Chinese with English abstract).

CARACCIOLO, L., LE PERA, E., MUTO, F. & PERRI, F. 2011. Sandstone petrology and mudstone geochemistry of the Peruc-Korycany Formation (Bohemian Cretaceous Basin, Czech Republic). *International Geology Review* **53**, 1003–31.

CHANG, L. H., WANG, X. Y., WANG, X. Z., ZHAO, B. X. & LIANG, H. J. 2007. Characteristics and evolution of thrust nappe structure in the Mohe Area, Daxing'anling. *Journal of Jilin University (Earth Science Edition)* **37**, 11–5 (in Chinese with English abstract).

CRITELLI, S. & INGERSOLL, R. V. 1994. Sandstone petrology and provenance of the Siwalik Group (northwestern Pakistan and western-southeastern Nepal). *Journal of Sedimentary Research* **64**, 815–23.

CRITELLI, S. & INGERSOLL, R. V. 1995. Interpretation of neovolcanic versus palaeovolcanic sand grains: an example from Miocene deep-marine sandstone of the Topanga Group (southern California). *Sedimentology* **42**, 783–804.

CRITELLI, S., MONGELLI, G., PERRI, F., MARTÍN-ALGARRA, A., MARTÍN-MARTÍN, M., PERRONE, V., DOMINICI, R., SONNINO, M. & ZAGHLOUL, M. N. 2008. Compositional and geochemical signatures for the sedimentary evolution of the Middle Triassic–Lower Jurassic continental redbeds from Western-Central Mediterranean Alpine chains. *Journal of Geology* **116**, 375–86.

CRITELLI, S., MUTO, F., TRIPODI, V. & PERRI, F. 2013. Link between thrust tectonics and sedimentation processes of stratigraphic sequences from the southern Apennines foreland basin system, Italy. *Rendiconti Online della Società Geologica Italiana* **25**, 21–42.

CROSDALE, P. J., SOROKIN, A. P., WOOLFE, K. J. & MACDONALD, D. I. M. 2002. Inertinite-rich Tertiary coals from the Zeya–Bureya Basin, Far Eastern Russia. *International Journal of Coal Geology* **51**, 215–35.

DICKINSON, W. R. 1985. Interpreting provenance relations from detrital modes of sandstones. In *Provenance of Arenites* (ed. G. G. Zuffa), pp. 333–61. Dordrecht: Reidel.

DICKINSON, W. R. 1988. Provenance and sediment dispersal in relation to paleotectonics and paleogeography of sedimentary basins. In *New Perspectives in Basin Analysis* (eds K. L. Kleinspehn & C. Paola), pp. 3–26. Springer.

DICKINSON, W. R., BEARD, L. S., BRAKENIRIDGE, G. R., ERJAVEC, J. L., FERGUSON, R. C., INMAN, K. F., KNEPP, R. A., LINDBERG, F. A. & RYBERG, P. T. 1983. Provenance of North American Phanerozoic sandstones in relation to tectonic setting. *Geological Society of America Bulletin* **94**, 222–35.

DICKINSON, W. R. & SUCZEK, C. A. 1979. Plate tectonics and sandstone compositions. *American Association of Petroleum Geologists Bulletin* **63**, 2164–82.

FANG, S. H., GUO, S. J., WU, C. D., ZHANG, Z. C., WANG, M. N. & YUAN, Q. D. 2006. Jurassic clastic composition in the Southern Junggar Basin, Northwest China: implications for basin-range pattern and tectonic attributes. *Acta Geologica Sinica* **80**, 196–209 (in Chinese with English abstract).

FANG, S. H., JIA, C. Z., SONG, Y., GUO, Z. J., YUAN, S. W. & WANG, X. L. 2007*a*. Meso-Cenozoic tectonic events and structural constraints in the Southern Junggar basin: evidence from detrital compositions. *Chinese Journal of Geology* **81**, 753–65 (in Chinese with English abstract).

FANG, S. H., SONG, Y., JIA, C. Z., WANG, X. L. & YUAN, Q. D. 2007*b*. The Mesozoic-Cenozoic clastic composition of Bogda Area, Xinjiang: implications on the evolution of basin-range pattern. *Acta Geologica Sinica* **81**, 1229–37 (in Chinese with English abstract).

FOLK, R. L. 1974. *Petrology of Sedimentary Rocks*. Austin, Texas: Hemphill's, 182 pp.

GE, W. C., SUI, Z. M., WU, F. Y., ZHANG, J. H. & XU, X. C. 2007. Zircon U-Pb ages, Hf isotopic characteristics and their implications of the Early Paleozoic granites in the northeastern Da Hinggan Mts., northeastern China. *Acta Petrologica Sinica* **23**, 423–40 (in Chinese with English abstract).

GE, W. C., WU, F. Y., ZHOU, C. Y. & RAHMAN, A. A. A. 2005. Emplacement age of the Tahe granite and its constraint on the tectonic nature of the Erguna block in the northern part of the Daxing an Range. *Chinese Science Bulletin* **50**, 1239–47 (in Chinese with English abstract).

GHAZI, S. & MOUNTNEY, N. P. 2011. Petrography and provenance of the Early Permian Fluvial Warchha Sandstone,

Salt Range, Pakistan. *Sedimentary Geology* **233**, 88–110.

GRAHAM, S. A., HENDRIX, M. S., WANG, L. B. & CARROL, A. R. 1993. Collision successor basin of western China: impact of tectonic inheritance on sand composition. *Geological Society of America Bulletin* **105**, 323–44.

GRAY, M. B. & ZEITLER, P. K. 1997. Comparison of clastic wedge provenance in the Appalachian foreland using U-Pb ages of detrital zircons. *Tectonics* **16**, 151–60.

HE, Z. J., LI, J. T., MO, S. G. & SOROKIN, A. A. 2003. Tectonic setting of geochemical characteristics and provenance analysis of the sandstones in Mohe foreland basin. *Science in China (Series D)* **33**, 1219–26 (in Chinese with English abstract).

HE, Z. H., WANG, Y. F. & HOU, W. 2008. Geochemistry and provenance analysis of the Middle Jurassic sandstones in the Mohe Basin, Heilongjiang. *Sedimentary Geology and Tethyan Geology* **28**, 93–100 (in Chinese with English abstract).

HENDRIX, M. S. 2000. Evolution of Mesozoic sandstone compositions, southern Junggar, northern Tarim, and western Tumpan basin northwest China: a detrital record of the ancestral Tian Shan. *Journal of Sedimentary Research* **70**, 520–32.

HENDRIX, M. S., GRANHAM, S. A., CARROLL, A. R., SOBLE, E. R., MCNIGHT, C. L., SCHLEIN, B. J. & WANG, Z. X. 1992. Sedimentary record and climatic implications of recurrent deformation in the Tian Shan: evidence from Mesozoic strata of the north Tarim, south Junggar, and Turpan basins, northwest China. *Geological Society of America Bulletin* **104**, 53–79.

HOU, W., LIU, Z. J., HE, Y. P., HE, Z. H. & ZHANG, L. 2010a. Provenance analysis of Middle Jurassic sediments and its geological significance in Mohe Basin. *Journal of Jilin University (Earth Science Edition)* **40**, 286–97 (in Chinese with English abstract).

HOU, W., LIU, Z. J., HE, Y. P., HE, Z. H., ZHANG, Y. Q. & ZHANG, L. 2010b. Provenance analysis of Upper Jurassic and its geological significances in Mohe Basin. *Geological Review* **56**, 71–9 (in Chinese with English abstract).

INGERSOLL, R. V. 1988. Tectonics of sedimentary basins. *Geological Society of America Bulletin* **100**, 1704–19.

INGERSOLL, R. V., FULLARD, T. F., FORD, R. L., GRIMM, J. P., PICKLE, J. D. & SARES, S. W. 1984. The effect of grain size on detrital modes: a test of the Gazzi-Dickinson point counting method. *Journal of Sedimentary Petrology* **54**, 103–16.

INGERSOLL, R. V. & SUCZEK, C. A. 1979. Petrology and provenance of Neogene sand from Nicobar and Bengal fans. DSDP sites 211 and 218. *Journal of Sedimentary Petrology* **49**, 1217–28.

LEE, Y. I. & SHEEN, D. H. 1998. Detrital modes of the Pyeongan Supergroup (Late Carboniferous–Early Triassic) sandstones in the Samcheog coalfield, Korea: implications for provenance and tectonic setting. *Sedimentary Geology* **119**, 219–38.

LI, C. L. 2007. *Structural characteristic, tectonic evolution and basin dynamics of Mohe Basin.* Ph.D. thesis, College of Earth Science, China University of Geosciences, Beijing. Published thesis. pp. 24–45 (in Chinese with English abstract).

LI, Z., SONG, W. J., PENG, S, T., WANG, D. X. & ZHANG, Z. P. 2004a. Mesozoic– Cenozoic tectonic relationships between the Kuqa subbasin and Tian Shan, northwest China: constraints from depositional records. *Sedimentary Geology* **172**, 223–49.

LI, Z., WANG, D. X., LIN, W. & WANG, Q. C. 2004b. Mesozoic-Cenozoic clastic composition in Kuqa depression, northwest China: implication for provenance types and tectonic attributes. *Acta Petrologica Sinica* **20**, 655–66 (in Chinese with English abstract).

LIN, C. S., YANG, H. J., LIU, J. Y., RUI, Z. F., CAI, Z. Z. & ZHU, Y. F. 2012. Distribution and erosion of the Paleozoic tectonic unconformities in the Tarim Basin, Northwest China: significance for the evolution of paleo-uplifts and tectonic geography during deformation. *Journal of Asian Earth Sciences* **46**, 1–19.

LIU, Y. Q., WANG, Z. X., JIN, X. C., LI, T. & LI, Y. 2004. Evolution, chronology and depositional effect of uplifting in the eastern sector of the Tianshan Mountains. *Acta Geologica Sinica* **78**, 319–31 (in Chinese with English abstract).

LU, F. X. & SANG, L. 2002. Geological. pp. 162–78. Geological Publishing House of Beijing, Special Publication no. 116 (in Chinese).

MARENSSI, S. A., NET, L. I. & SANTILLANA, S. N. 2002. Provenance, environmental and paleogeographic controls on sandstone composition in an incised-valley system: the Eocene La Meseta Formation, Seymour Island, Antarctica. *Sedimentary Geology* **150**, 301–21.

MO, S. G., HAN, M. L. & LI, J. T. 2005. Compositions and orogenic processes of Mongolia-Okhotsk Orogen. *Journal of Shandong University of Science and Technology (Natural Science)* **24**, 50–64 (in Chinese with English abstract).

MORTON, A. C. & HALLSWORTH, C. 1994. Identifying provenance specific features of detrital heavy mineral assemblages in sandstones. *Sedimentary Geology* **90**, 241–56.

PERRI, F., CIRRINCIONE, R., CRITELLI, S., MAZZOLENI, P. & PAPPALARDO, A. 2008. Clay mineral assemblages and sandstone compositions of the Mesozoic Longobucco Group (north-eastern Calabria): implication for burial history and diagenetic evolution. *International Geology Review* **50**, 1116–31.

PERRI, F., CRITELLI, S., CAVALCANTE, F., MONGELLI, G., DOMINICI, R., SONNINO, M. & DE ROSA, R. 2012. Provenance signatures for the Miocene volcaniclastic succession of the Tufiti di Tusa Formation, southern Apennines, Italy. *Geological Magazine* **149**, 423–42.

PERRI, F., CRITELLI, S., MARTÍN-ALGARRA, A., MARTÍN-MARTÍN, M., PERRONE, V., MONGELLI, G. & ZATTIN, M. 2013. Triassic redbeds in the Malaguide Complex (Betic Cordillera – Spain): petrography, geochemistry, and geodynamic implications. *Earth-Science Reviews* **117**, 1–28.

PERRI, F., CRITELLI, S., MONGELLI, G. & CULLERS, R. L. 2011. Sedimentary evolution of the Mesozoic continental redbeds using geochemical and mineralogical tools: the case of Upper Triassic to Lowermost Jurassic M.te di Gioiosa mudstones (Sicily, southern Italy). *International Journal of Earth Sciences* **100**, 1569–87.

RIESER, A. B., NEUBAUER, F., LIU, Y. J. & GE, X. H. 2005. Sandstone provenance of north-western sectors of the intracontinental Cenozoic Qaidam basin, western China: tectonic vs. climatic control. *Sedimentary Geology* **177**, 1–18.

SHAO, J. D., TAN, Q., WANG, H., ZHANG, M. & HE, H. Y. 2011. The Mesozoic strata and the Jurassic-Cretaceous boundary in the Daxinganling Region. *Geology and Resources* **20** (1), 4–11.

SUN, G. R., LI, Y. C. & ZHANG, Y. 2002. The basement tectonics of Erguna massif. *Geology and Resources* **11**, 129–39 (in Chinese with English abstract).

WANG, C. W., SUN, Y. W., LI, N., ZHAO, G. W. & MA, X. Q. 2009. Tectonic implications of Late Paleozoic stratigraphic distribution in Northeast China and adjacent region. *Science in China (Series D) – Earth Science* **52**, 619–26.

WU, G. Y., FENG, Z. Q., YANG, J. G., WANG, Z. J., ZHANG, L. G. & GUO, Q. X. 2006. Tectonic setting and geological evolution of Mohe basin in Northeast China. *Oil & Gas Geology* **27**, 528–35 (in Chinese with English abstract).

WU, G., SUN, F. Y., ZHAO, C. S., LI, Z. T., ZHAO, A. L., PANG, Q. B. & LI, G. Y. 2005. Discovery of the Early Paleozoic post-collisional granites in northern margin of the Erguna massif and its geological significance. *Chinese Science Bulletin* **50**, 2278–88 (in Chinese with English abstract).

WU, H. Y., WANG, S. H. & YANG, J. G. 2004. Analysis of exploration potential in surrounding basins of Daqing Oilfield. *China Petroleum Exploration* **4**, 23–31 (in Chinese with English abstract).

WU, H. Y., YANG, J. G., HUANG, Q. H. & LIU, W. L. 2003. Sequence and age of the Mesozoic strata of Mohe Basin. *Journal of Stratigraphy* **27**, 193–8 (in Chinese with English abstract).

XIE, M. Q. 2000. The cohesive slab structures and their driving mechanism–tectonics evolutions in the Northeast China and neighboring areas, pp. 66–70. Science Press of Beijing, Special Publication no. 134 (in Chinese).

XIN, R. C., WU, H. Y. & YANG, J. G. 2003. Upper Jurassic sequence-stratigraphic framework of the Mohe Basin. *Journal of Stratigraphy* **27**, 198–204 (in Chinese with English abstract).

XU, G. G. & YAN, H. Q. 1996. Accretionary tectonics in the Northeast of Russia. *Global Geology* **15**, 35–8 (in Chinese).

YAN, Y., LIN, G., WANG, Y. J. & GUO, F. 2002. The indication of continental detrital sediment to tectonic setting. *Advances in Earth Sciences* **17**, 85–90 (in Chinese with English abstract).

ZAGHLOUL, M. N., CRITELLI, S., PERRI, F., MONGELLI, G., PERRONE, V., SONNINO, M., TUCKER, M., AIELLO, M. & VENTIMIGLIA, C. 2010. Depositional systems, composition and geochemistry of Triassic rifted-continental margin redbeds of Internal Rif Chain, Morocco. *Sedimentology* **57**, 312–50.

ZENG, Y. F. & XIA, W. J. 1998. Petrology, pp. 212–25. Geological Publishing House of Beijing, Special Publication no.112 (in Chinese).

ZHANG, S., LIN, C. M., WU, C. D. & YANG, J. G. 2003. Tectonic characteristics and basin evolution of the Mohe Basin, Heilongjiang Province. *Geological Journal of China University* **9**, 411–8 (in Chinese with English abstract).